



■ KNEE

The anterolateral ligament is a secondary stabilizer in the knee joint

A VALIDATED COMPUTATIONAL MODEL OF THE BIOMECHANICAL EFFECTS OF A DEFICIENT ANTERIOR CRUCIATE LIGAMENT AND ANTEROLATERAL LIGAMENT ON KNEE JOINT KINEMATICS

**K-T. Kang,
Y-G. Koh,
K-M. Park,
C-H. Choi,
M. Jung,
J. Shin,
S-H. Kim**

Department of
Orthopedic Surgery,
Arthroscopy and Joint
Research Institute,
Yonsei University
College of Medicine,
Seoul, South Korea

Objectives

The aim of this study was to investigate the biomechanical effect of the anterolateral ligament (ALL), anterior cruciate ligament (ACL), or both ALL and ACL on kinematics under dynamic loading conditions using dynamic simulation subject-specific knee models.

Methods

Five subject-specific musculoskeletal models were validated with computationally predicted muscle activation, electromyography data, and previous experimental data to analyze effects of the ALL and ACL on knee kinematics under gait and squat loading conditions.

Results

Anterior translation (AT) significantly increased with deficiency of the ACL, ALL, or both structures under gait cycle loading. Internal rotation (IR) significantly increased with deficiency of both the ACL and ALL under gait and squat loading conditions. However, the deficiency of ALL was not significant in the increase of AT, but it was significant in the increase of IR under the squat loading condition.

Conclusion

The results of this study confirm that the ALL is an important lateral knee structure for knee joint stability. The ALL is a secondary stabilizer relative to the ACL under simulated gait and squat loading conditions.

Cite this article: *Bone Joint Res* 2019;8:509–517.

Keywords: Anterolateral ligament, Anterior cruciate ligament, Computational analysis

Article focus

■ Assessment and comparison of the anterolateral ligament (ALL), anterior cruciate ligament (ACL), or both ALL and ACL on kinematics under dynamic loading conditions.

Key messages

- ALL is a secondary stabilizer relative to the ACL under simulated gait and squat loading conditions.
- ACL and ALL work independently and synergically in the knee joint under gait and squat loading conditions.

Strengths and limitations

- Our simulation was performed using five different models, rather than using a single representative model.

- Computational analysis study was carried out without clinical data.

Introduction

Injury of the anterolateral complex in the knee joint is often accompanied by anterior cruciate ligament (ACL) rupture.¹⁻³ This is usually treated surgically using standard procedures that have improved over several decades.⁴⁻⁷ However, residual anterolateral rotational instabilities (ALRI) negatively correlate with functional outcomes and remain challenging to treat.^{4,8,9} Despite the inherent limitations of biomechanical studies, it has been suggested that the ALL may contribute to the anterolateral stability of the knee joint as a secondary stabilizer by preventing anterolateral subluxation of the proximal tibia on the femur.^{4,8,10} Several studies have reported

Correspondence should be sent to
S-H. Kim; email:
orthohwanbm@gmail.com

doi: 10.1302/2046-3758.811.
BJR-2019-0103.R1

Bone Joint Res 2019;8:509–517.

that the ALL is a well-defined and distinct ligamentous structure of the knee joint.^{4,11,12} Histological examination revealed that the ALL consists of compact collagen fibres in a parallel orientation, compatible with ligamentous or tendinous tissues.¹² The presence of the ALL in previous anatomical studies varied from 83% to 100%,¹³ but it should be noted that the ALL designation has been used inconsistently with regard to its precise insertions.^{4,14,15}

A correlation between ALL injuries and ACL ruptures has been postulated to underlie anterolateral rotatory instability, leading to a positive pivot-shift test result.^{4,8} In a previous biomechanical study, ALL damage led to knee instability at high flexion. Furthermore, other studies suggested that the ALL is responsible for the Segond avulsion fracture, a well-known radiological sign of an ACL tear.¹⁶⁻¹⁸ Simultaneous ALL and ACL tears have been theorized to occur due to a common mechanism of injury involving excessive internal rotation (IR) torque.² Parsons et al¹⁶ performed a biomechanical study to investigate the function of the ALL. They reported that the ALL made a large contribution to IR stability in flexion, but contributed minimally to anterior tibial translational stability from 0° to 90° of flexion.¹⁶ Saiegh et al¹⁹ found that dissection of the ALL in an ACL-deficient knee did not increase instability in a cadaveric model. Schon et al²⁰ suggested that an anatomical ALL reconstruction in conjunction with an ACL reconstruction resulted in joint overconstraint. Therefore, the ability of combined ACL and ALL reconstructions to safely restore native joint kinematics without causing joint overconstraint is unclear.²⁰ However, Thein et al,²¹ based on a biomechanical study, found that the ALL carried minimal load during the pivot shift, Lachman, and anterior drawer tests. Furthermore, Tavlo et al¹¹ found that ALL was a significant stabilizer of tibial inward rotation. Reconstruction of a torn ALL in ACL-reconstructed knees significantly improved inward rotational stability. As can be seen from the above review of previous research, the biomechanical effects of the ALL are still controversial. However, to the best of our knowledge, the literature has seldom investigated the kinematic changes in response to deficiency of the ALL, ACL, or both ligaments during daily dynamic activities such as walking and squatting.

The objective of this study was to develop and validate a subject-specific musculoskeletal (MSK) model with 12-degrees-of-freedom motion at both the tibiofemoral (TF) and patellofemoral (PF) joints based on data from four healthy male subjects and one healthy female subject. First, to validate the computational model, predicted muscle activation and corresponding electromyography (EMG) recordings were compared. In addition, the anterior drawer test results for an intact condition, and for both ACL and ALL deficiency, were compared with previous experimental results. Second, kinematics were compared for anteroposterior (AP) translations and internal-external (IE) rotations with respect to a deficient

ACL, deficient ALL, or deficient ACL and ALL under gait and squat loading conditions. We hypothesized that the ALL is an important lateral knee structure for knee joint stability during daily dynamic activity.

Patients and Methods

Experimental procedures. After receiving approval from the hospital's institutional review board (3-2016-0271) and written informed consent from all subjects, subject-specific data were used to develop subject-specific MSK models, and EMG sensors were used for motion capture. Four male subjects and one female subject who had no previous medical history of lower limb problems participated in this study. The mean age, height, and weight of subjects were 33.0 years (SD 4.4; 26 to 36), 175 cm (SD 7.4; 163 to 182), and 75.6 kg (SD 6.7; 65 to 83), respectively. The subjects performed gait and squatting activities, and ground reaction forces were measured using a force plate. In addition, tracks of marker locations were measured using a 3D motion capture system (Vicon, Oxford, United Kingdom) (Fig. 1). EMG signals were recorded from the following muscles using an EMG sensor (Delsys, Boston, Massachusetts): gluteus maximus, rectus femoris, vastus lateralis, biceps femoris, semimembranosus, gastrocnemius medialis, tibialis anterior, and soleus medialis. Raw data from the EMG signals were transformed into muscle activation data by root mean square analysis.²²

Computational model. The five subject-specific models were developed using AnyBody version 6.0.5 (AnyBody Technology, Aalborg, Denmark), a commercial software package for MSK simulation analysis. The generic lower limb MSK model is based on the Twente Lower Extremity Model anthropometric database.²³ The MSK model is actuated by approximately 160 muscle units. It has been previously validated for predicting muscle and joint reaction forces in human lower limbs during locomotion.²⁴⁻²⁶

3D bone and soft-tissue models were reconstructed from CT and MRI scans in our previous study.²⁷⁻²⁹ By using 3D femoral and tibial models of the five subjects, the femur and tibia in AnyBody were scaled with non-linear radial basis functions as scaling laws. The remaining parts were scaled using an optimization scheme that minimizes the difference between the model markers and recorded marker positions. The knee joint in this study was considered to have 12 degrees of freedom (TF, six; PF, six). The hip and ankle joints were considered to have three and two degrees of freedom, respectively.

Ligament insertion points were also observed in the MRI sets and descriptions can be found in the literature. Two experienced orthopaedic surgeons (YGK and SHK) determined the locations of the ligaments independently.³⁰⁻³⁶ The attachment points in AnyBody model were modified using the subject-specific attachment sites. As shown in Figure 2, the following 21 ligament bundles were modelled: the ACL (anteromedial bundle of the ACL (aACL),

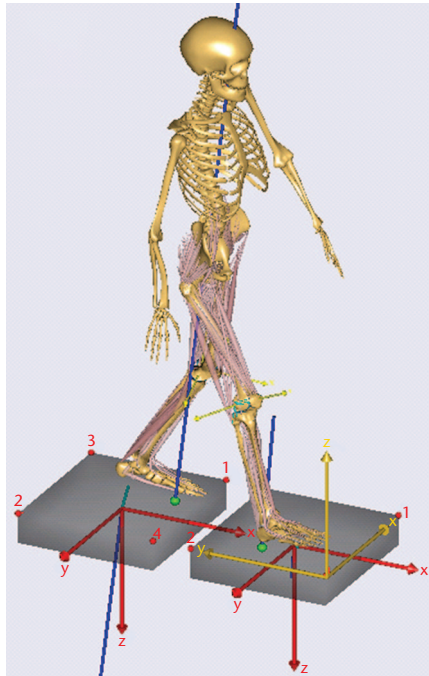


Fig. 1a

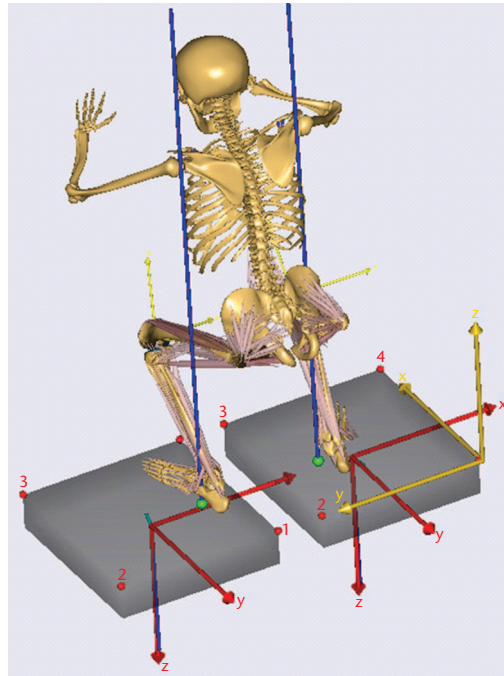


Fig. 1b

Schematic of subject-specific musculoskeletal models during a) gait and b) squat loading conditions.

posterolateral bundle of the ACL (pACL); posterior cruciate ligament (PCL; anterolateral bundle of the PCL (aPCL), posteromedial bundle of the PCL (pPCL)), anterolateral ligament (ALL); lateral collateral ligament (LCL); popliteofibular ligament (PFL); medial collateral ligament (MCL; anterior portion (aMCL), central portion (cMCL), posterior portion (pMCL)); deep medial collateral ligament (anterior portion (aCM), posterior portion (pCM)); medial and lateral posterior capsule (mCAP and lCAP, respectively); oblique popliteal ligament (OPL); medial PF ligament (superior (sMPFL), middle (mMPFL), inferior (iMPFL)); and lateral PF ligament (superior (sLPFL), middle (mLPFL), inferior (iLPFL)).

The stiffness-force relationship of the ligaments in this model were defined as follows to produce non-linear elastic characteristics with a slack region.³⁷

$$f(\varepsilon) = \begin{cases} \frac{k\varepsilon^2}{4\varepsilon_1}, & 0 \leq \varepsilon \leq 2\varepsilon_1 \\ k(\varepsilon - \varepsilon_1), & \varepsilon > 2\varepsilon_1 \\ 0, & \varepsilon < 0 \end{cases}$$

$$\varepsilon = \frac{l - l_0}{l_0}$$

$$l_0 = \frac{l_r}{\varepsilon_r + 1}$$

Where $f(\varepsilon)$ is the current force, k is the stiffness, ε is the strain, and ε_1 was assumed to be constant at 0.03. The ligament bundle slack length, l_0 , was calculated from the reference bundle length, l_r , and the reference strain, ε_r , in the upright reference position. Most of the stiffness and reference strain values were adopted from the literature, with some modifications.³⁷⁻³⁹

Menisci were modelled as linear springs to simulate their equivalent resistance.⁴⁰ A wrapping surface comprising a cylinder and an ellipsoid was applied to prevent penetration of bone by ligaments. One-to-three wrapping surfaces were applied to each ligament to wrap the geometry of the bone. Figure 2 shows three rigid-rigid standard tessellation language (STL)-based contacts defined in the TF and PF joints. Three deformable contact models were defined between the femoral and tibial components, and between the femoral component and patellar button. These contact forces were proportional to the penetration volume and so-called pressure module.³⁸

Inverse dynamic simulation and loading conditions. Before running the inverse dynamic analysis, the kinematics of each trial were calculated on the basis of motion capture data. Kinematic optimization was used for this purpose. To optimize the kinematic model parameters, ground reaction forces and motion capture marker trajectory data were imported into AnyBody. The optimization objective was to minimize the difference between the AnyBody model marker trajectories and the motion capture marker trajectories. After kinematic optimization, inverse dynamic analysis was performed. Muscle

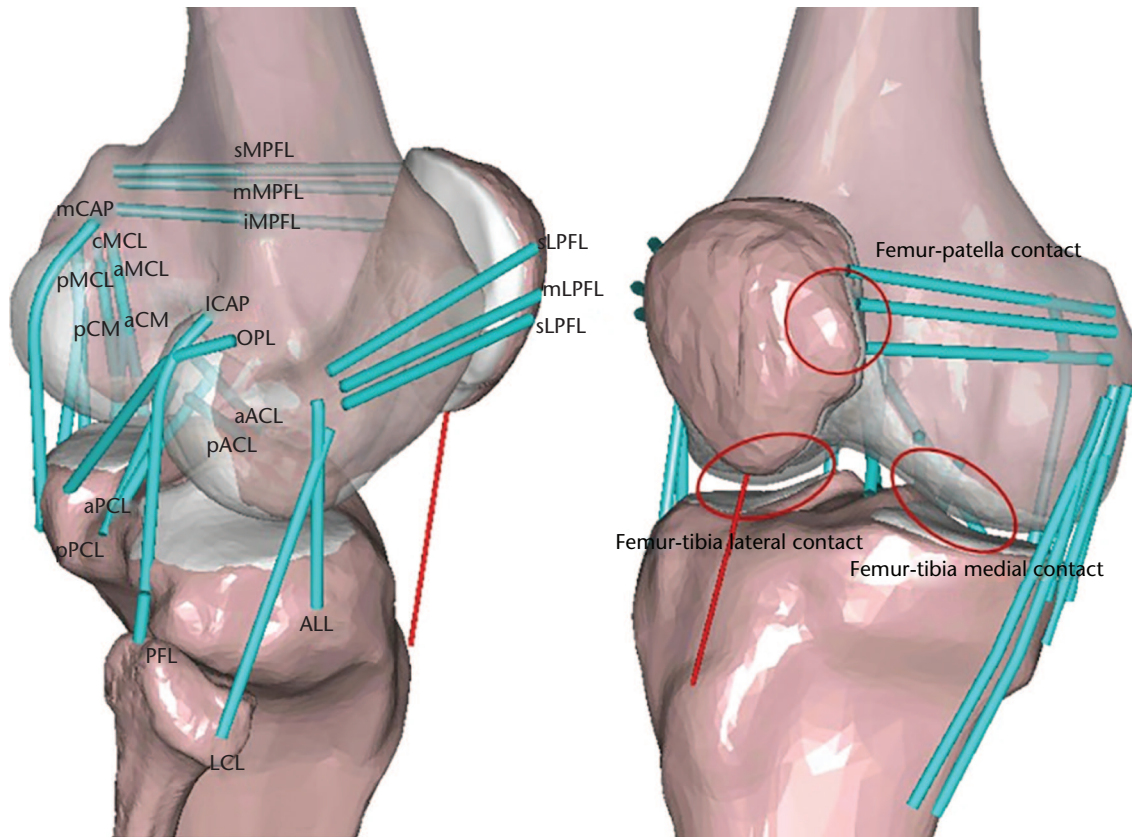


Fig. 2

Schematic of subject-specific musculoskeletal model during gait and squat conditions with contact conditions and 21 ligament bundles: anteromedial bundle (aACL) and posterolateral bundle (pACL) of the anterior cruciate ligament; anterolateral bundle (aPCL) and posteromedial bundle of the posterior cruciate ligament (pPCL); anterolateral ligament (ALL); lateral collateral ligament (LCL); popliteofibular ligament (PFL); anterior portion (aMCL), central portion (cMCL), and posterior portion (pMCL) of the medial collateral ligament; anterior portion (aCM) and posterior portion (pCM) of the deep medial collateral ligament; medial (mCAP) and lateral (ICAP) posterior capsules; oblique popliteal ligament (OPL); superior (sMPFL), middle (mMPFL), and inferior (iMPFL) medial patellofemoral ligament; and superior (sLPFL), middle (mLPFL), and inferior (iLPFL) lateral patellofemoral ligament.

recruitment criterion used in this study was cubic polynomial. To assess the predictive accuracy of the models, predicted activations for major muscles were compared with EMG signals. The anterior tibial translations in the anterior drawer test under the conditions of an intact condition, and for deficient ACL and ALL with 88 N of force at 0°, 30°, 60°, and 90° of flexion were compared with previous experimental data.^{20,41}

To define the influence of resection of the ALL and ACL structures on the ACL and ALL, respectively, AP translation, and IE rotation with deficiency of the ALL, ACL, and both ligaments for individual components were compared with the intact condition under gait and squat loading conditions.

Statistical analysis. Single cycles of gait and squatting were divided into 11 timepoints (0.0 to 1.0 phases). Calculated kinematic data in each simulated model were compared with the corresponding simulation data from the same knee at the same phase of the cycle. Non-parametric repeated measures Friedman tests and *post hoc* comparisons were performed using a Wilcoxon's signed-rank test with Holm correction to compare results

obtained under ligament deficient status and the intact knee condition. Statistical analyses were performed using SPSS for Windows (version 20.0.0; IBM, Armonk, New York). Statistical significance was set at $p < 0.05$ for all comparisons.

Results

Comparison of anterior drawer and EMG experimental results with the predicted computational model. The greatest muscle excitation pattern activities predicted from the five computational models showed consistency with the transformed EMG measurements under the gait and squat loading conditions shown in Supplementary Figures a and b. For the intact condition, and for the deficient ACL and ALL models, the mean values for the anterior translation (AT) from computational simulation were within the range of values from previous experimental studies (Fig. 3).

Comparison of kinematics with respect to ACL, ALL, and both ACL and ALL ligament deficiency under gait and squat loading conditions. Figure 4 shows AP translation and IE rotation for a deficient ACL, ALL, and both ligaments

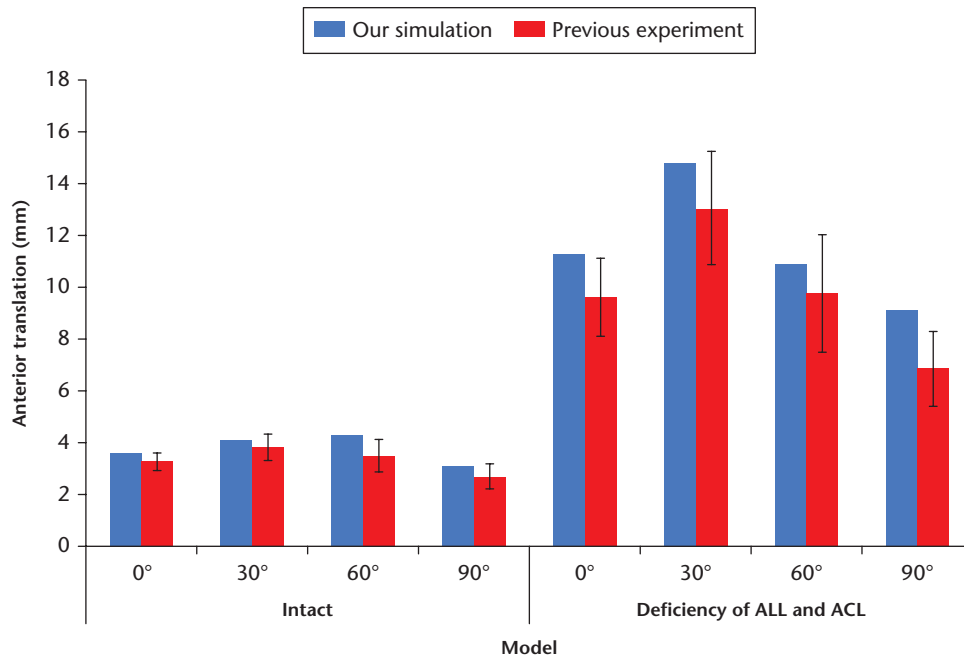


Fig. 3

Comparison of the anterior tibial translations in the anterior drawer test between the intact and the anterolateral ligament (ALL) and anterior cruciate ligament (ACL) deficient conditions.

under gait cycle loading.⁴² The mean maximum difference was 3.4 mm more in anterior tibial translation with deficiency of the ACL than the intact condition at the 0.3 period during the stance phase, which was significant. The mean maximum difference was 3.9 mm more in anterior tibial translation with deficiency of the ALL than the intact condition at the 0.3 to 0.4 periods during the stance phase, which was significant. There was greater anterior tibial translation with deficiency of both ligaments under gait loading, suggesting that the ACL and ALL interact synergistically. The mean maximum difference was 5.8 mm more in anterior tibial translation with deficiency of both ligaments than the intact condition at the 0.2 to 0.4 periods during the stance phase, which was significant. Mean maximum IR with respect to deficiency of the ACL, ALL, or both ligaments was 2.6°, 1.8°, and 6.6° compared with the intact condition under gait loading condition. The deficiency of ACL (0.1 to 0.6 period) and both ligaments (0.1 to 0.8 period) was significant on the increased IR during gait cycle, not in the deficiency of ALL.

AP translation and IE rotation for deficient ACL, ALL, and deficient ACL and ALL conditions under squat cycle loading are shown in Figure 5.⁴² Anterior tibial translation was significantly influenced by a deficient ACL for the entire cycle of squat loading. However, there was no difference in anterior tibial translation with deficiency of the ALL during squat loading conditions. IR significantly increased during low flexion under squat loading for a deficiency of the ACL, while IR significantly increased during high flexion under squat loading cycle for a deficiency

of the ALL. The AT and IR with deficiency of both ligaments significantly increased compared with intact condition during squat loading condition.

Discussion

Our results indicate that the ALL is an important lateral knee structure for knee joint stability under gait cycle loading. In addition, ALL is a secondary stabilizer that works together with the ACL under simulated gait and squat loading.

Most previous *in vitro* studies have performed sectioning of the ACL followed by the ALL, and did not evaluate if the ALL could function as a stabilizer independently of the ACL.^{11,19-21,43} In addition, *in vitro* biomechanical studies are usually performed with cadavers of elderly people. Thus, if loads are repeatedly exerted for *in vitro* mechanical testing, not only loosening between the specimen and device, but also some attenuation of the tissue itself may occur.⁴⁴ Computational knee joint models enable some of the disadvantages of *in vitro* experimental studies, such as the limitations of cadaveric specimens under quasistatic loading conditions, to be overcome. *In vivo* kinematic studies are often performed postoperatively and the results then compared with those of a different group evaluated preoperatively.^{11,45} By computational simulation of subjects, the effects of deficiency of the ACL or ALL on the validated subject-specific models could be determined and effects of variables such as weight, height, bony geometry, and ligament properties excluded.

Deficiency of the ALL had as great an influence on AT as deficiency of the ACL during stance phase under gait

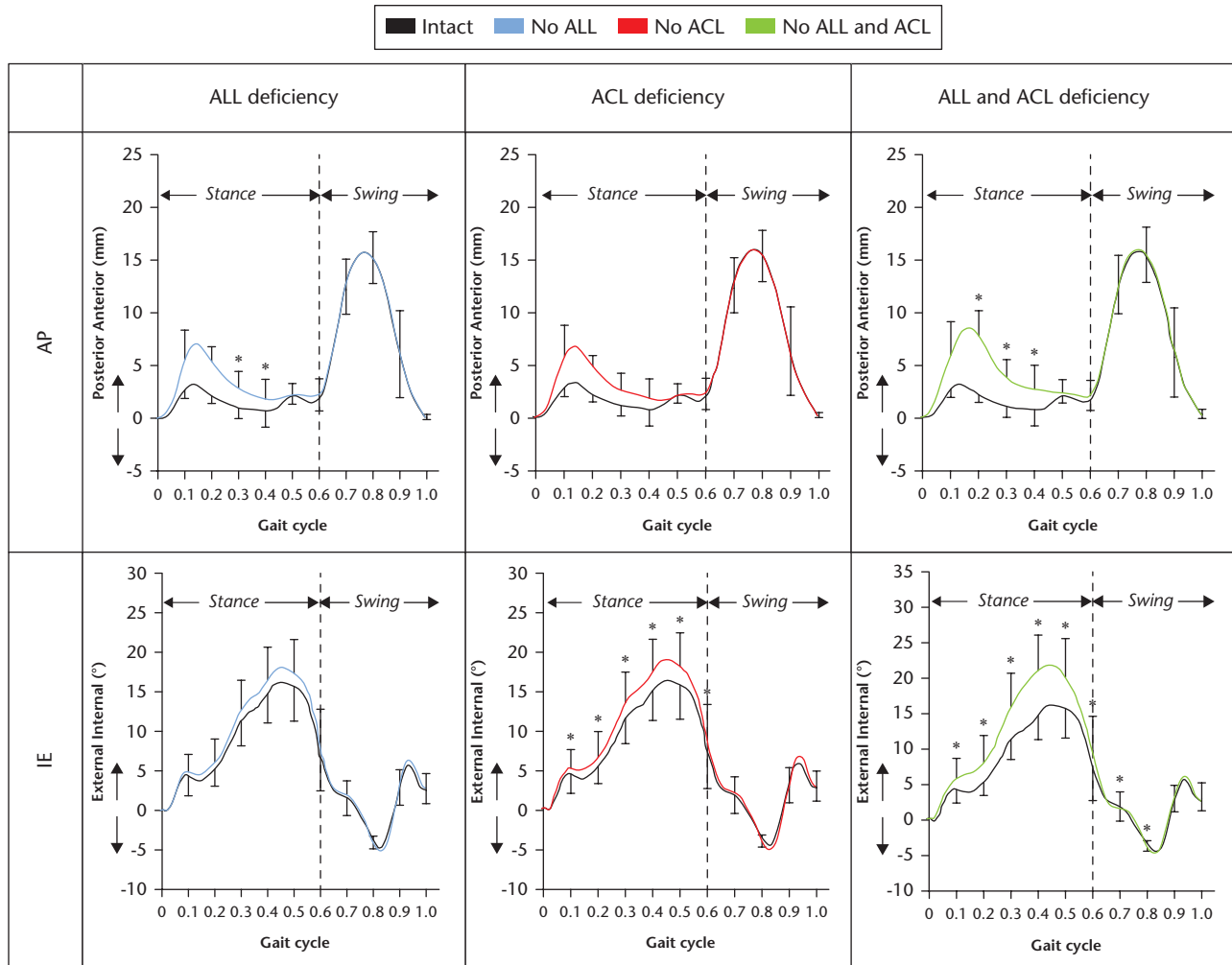


Fig. 4

Mean (SD) anteroposterior translation (AP) and internal–external (IE) rotation under gait cycle condition for deficiency of anterolateral ligament (ALL), anterior cruciate ligament (ACL), and both ALL and ACL.⁴² *Statistically significant.

loading. Our findings support a synergistic interaction between the ACL and ALL; the mean of AP translation and IE rotation increased by 166% and 35%, respectively, with deficiency of both ACL and ALL under gait loading. The mean AP translations increased by 108% and 120%, respectively, for deficiency of the ACL and ALL, while the mean IE rotations increased by 16% and 12%, respectively, for deficiency of the ACL and ALL. The sectioning order of the ACL and ALL did not influence their effect on AP translation and IE rotation, which suggests that the ALL and ACL function independently and synergistically. Ruiz et al⁴⁶ also found that the order of the sections did not have an effect on the total increase in IR and reported a similar trend to our results. Our study reinforces the importance of the ALL as an anterolateral structure.⁴³ In addition, our data demonstrate that the ALL is a major stabilizer of rotation, and also to a lesser extent of AP stability, under squat loading. AP translation was not influenced by deficiency of the ALL under squat loading. The effects of ALL deficiency on AP translation were consistent

with those reported in previous studies, which suggests that the ALL is an important second stabilizer under squat loading conditions.⁴¹ A previous study demonstrated that the contribution of the ALL during IR increased markedly with respect to flexion, whereas that of the ACL decreased significantly. At knee flexion angles greater than 30°, the contribution of the ALL exceeded that of the ACL. The authors of the previous study concluded that the ALL is an important stabilizer of IR at flexion angles greater than 35°.¹⁶ Deficiency of the ACL led to an increase in IR at full extension and lower flexion angles under squat loading. However, deficiency of the ALL resulted in an increase in IE rotation under squat loading, especially for high flexion angles. Furthermore, with deficiency of both ACL and ALL ligaments, IE rotation increased throughout all flexion angles compared with the intact condition under squat loading. Several cadaveric studies have shown a role for the ALL in IE rotation control, consistent with our findings.^{11,16,21,41,43,47} We demonstrated that the influence of the ALL on rotational stability is

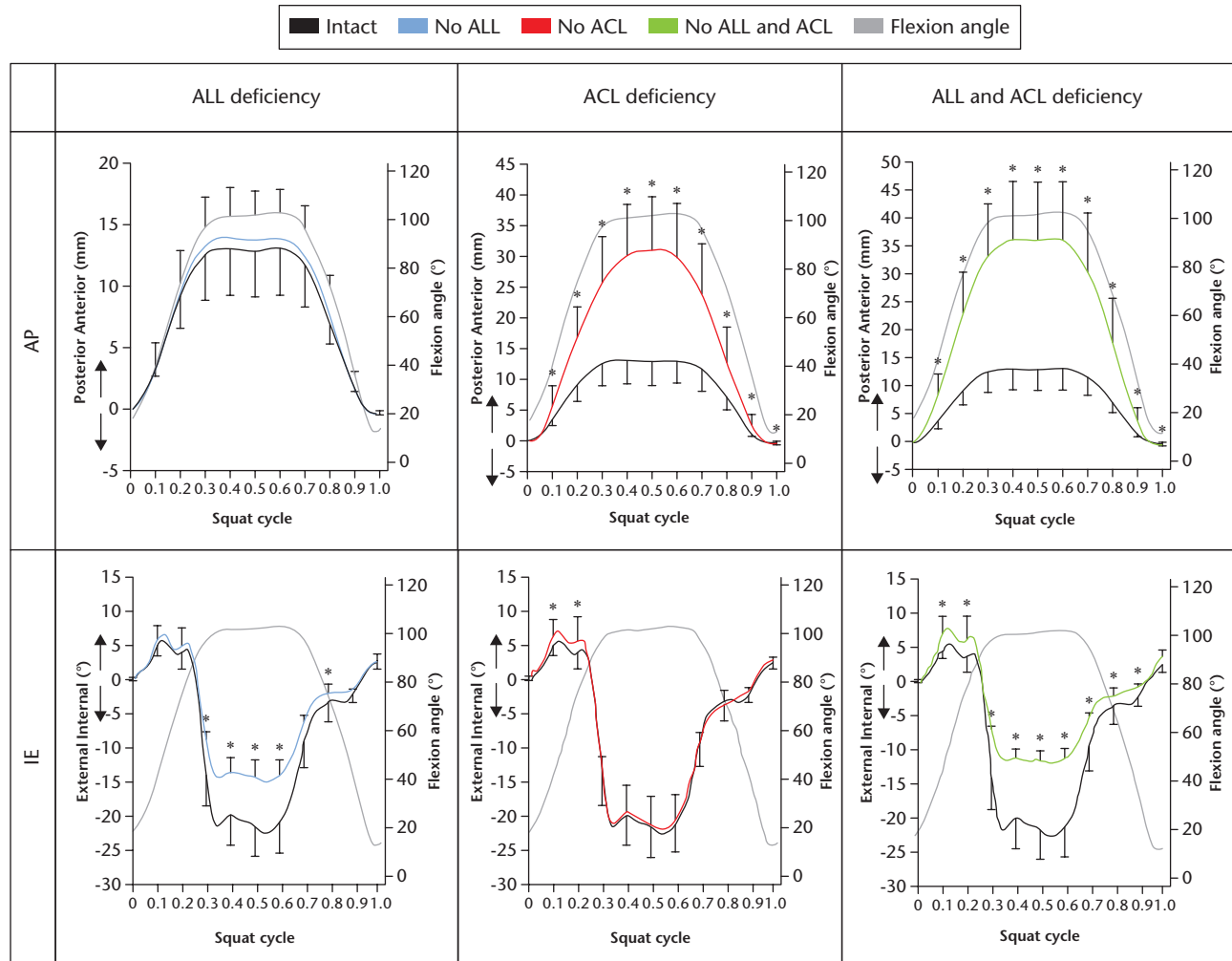


Fig. 5

Mean (SD) anteroposterior translation and internal–external rotation under squat cycle condition for deficiency of anterior cruciate ligament (ALL), anterior cruciate ligament (ACL), and both ALL and ACL.⁴² *Statistically significant.


greater than that of the ACL, which is supported by the fact that the lever arm from the rotatory axis of the knee joint in the middle of the medial compartment to the ACL is shorter than that to the ALL.¹¹ We also found that flexion degree influenced rotation opposite to both ligaments and the ACL, which contributed less to rotatory stability as flexion angle increased, while the ALL contributed more.

This study had some limitations. First, ligaments were modified into only two or three bundles. Secondly, the material properties of the ligaments in the model were extracted from the literature. Thirdly, the insertion point of the ALL in the models was modified manually to match the geometry of the respective subject's knee anatomy.^{48,49} The results could vary depending on the position of the ALL. Finally, there were differences between muscle force prediction and EMG measurements. Muscles were divided into multiple branches in the AnyBody MSK model, and the EMG signal was more related to the activity in large muscle groups closest to

the electrode. This may have contributed to large differences in the activation of some muscle groups.⁵⁰

In conclusion, the ALL is an important lateral knee structure for knee joint stability. The ALL is a secondary stabilizer relative to the ACL under simulated gait and squat loading conditions.

Supplementary Material

 Figures showing comparisons between measured and predicted muscle activations in five subject-specific musculoskeletal models, under normal gait and squat loading conditions.

References

- Irvine GB, Dias JJ, Finlay DB. Second fractures of the lateral tibial condyle: brief report. *J Bone Joint Surg [Br]* 1987;69-B:613-614.
- Hess T, Rupp S, Hopf T, Gleitz M, Liebler J. Lateral tibial avulsion fractures and disruptions to the anterior cruciate ligament. A clinical study of their incidence and correlation. *Clin Orthop Relat Res* 1994;303:193-197.
- Dietz GW, Wilcox DM, Montgomery JB. Second tibial condyle fracture: lateral capsular ligament avulsion. *Radiology* 1986;159:467-469.

4. **Dodds AL, Halewood C, Gupte CM, Williams A, Amis AA.** The anterolateral ligament: anatomy, length changes and association with the Segond fracture. *Bone Joint J* 2014;96-B:325-331.
5. **Queen RM.** Infographic: ACL injury reconstruction and recovery. *Bone Joint Res* 2017;6:621-622.
6. **Tawonsawatruk T, Sriwatananukulkit O, Himakhun W, Hemstapat W.** Comparison of pain behaviour and osteoarthritis progression between anterior cruciate ligament transection and osteochondral injury in rat models. *Bone Joint Res* 2018;7:244-251.
7. **Sato Y, Akagi R, Akatsu Y, et al.** The effect of femoral bone tunnel configuration on tendon-bone healing in an anterior cruciate ligament reconstruction: an animal study. *Bone Joint Res* 2018;7:327-335.
8. **Claes S, Vereecke E, Maes M, et al.** Anatomy of the anterolateral ligament of the knee. *J Anat* 2013;223:321-328.
9. **Rezansoff AJ, Caterine S, Spencer L, et al.** Radiographic landmarks for surgical reconstruction of the anterolateral ligament of the knee. *Knee Surg Sports Traumatol Arthrosc* 2015;23:3196-3201.
10. **Helito CP, Demange MK, Bonadio MB, et al.** Radiographic landmarks for locating the femoral origin and tibial insertion of the knee anterolateral ligament. *Am J Sports Med* 2014;42:2356-2362.
11. **Tavlo M, Eljaja S, Jensen JT, Siersma VD, Krosgaard MR.** The role of the anterolateral ligament in ACL insufficient and reconstructed knees on rotatory stability: a biomechanical study on human cadavers. *Scand J Med Sci Sports* 2016;26:960-966.
12. **Vincent JP, Magnussen RA, Gezmez F, et al.** The anterolateral ligament of the human knee: an anatomic and histologic study. *Knee Surg Sports Traumatol Arthrosc* 2012;20:147-152.
13. **Pomajzl R, Maerz T, Shams C, Guettler J, Bicos J.** A review of the anterolateral ligament of the knee: current knowledge regarding its incidence, anatomy, biomechanics, and surgical dissection. *Arthroscopy* 2015;31:583-591.
14. **Vieira EL, Vieira EA, da Silva RT, et al.** An anatomic study of the iliotibial tract. *Arthroscopy* 2007;23:269-274.
15. **Moorman CT III, LaPrade RF.** Anatomy and biomechanics of the posterolateral corner of the knee. *J Knee Surg* 2005;18:137-145.
16. **Parsons EM, Gee AO, Spiekerman C, Cavanagh PR.** The biomechanical function of the anterolateral ligament of the knee. *Am J Sports Med* 2015;43:669-674.
17. **Goldman AB, Pavlov H, Rubenstein D.** The Segond fracture of the proximal tibia: a small avulsion that reflects major ligamentous damage. *AJR Am J Roentgenol* 1988;151:1163-1167.
18. **Hatsushika D, Nimura A, Mochizuki T, et al.** Attachments of separate small bundles of human posterior cruciate ligament: an anatomic study. *Knee Surg Sports Traumatol Arthrosc* 2013;21:998-1004.
19. **Saiegh YA, Suero EM, Guenther D, et al.** Sectioning the anterolateral ligament did not increase tibiofemoral translation or rotation in an ACL-deficient cadaveric model. *Knee Surg Sports Traumatol Arthrosc* 2017;25:1086-1092.
20. **Schon JM, Moatshe G, Brady AW, et al.** Anatomic anterolateral ligament reconstruction of the knee leads to overconstraint at any fixation angle. *Am J Sports Med* 2016;44:2546-2556.
21. **Thein R, Boorman-Padgett J, Stone K, et al.** Biomechanical assessment of the anterolateral ligament of the knee: a secondary restraint in simulated tests of the pivot shift and of anterior stability. *J Bone Joint Surg [Am]* 2016;98-A:937-943.
22. **Lloyd DG, Besier TF.** An EMG-driven musculoskeletal model to estimate muscle forces and knee joint moments in vivo. *J Biomech* 2003;36:765-776.
23. **Klein Horsman MD, Koopman HF, van der Helm FC, Prosé LP, Veeger HE.** Morphological muscle and joint parameters for musculoskeletal modelling of the lower extremity. *Clin Biomech (Bristol, Avon)* 2007;22:239-247.
24. **Ali N, Andersen MS, Rasmussen J, Robertson DG, Rouhi G.** The application of musculoskeletal modeling to investigate gender bias in non-contact ACL injury rate during single-leg landings. *Comput Methods Biomech Biomed Engin* 2014;17:1602-1616.
25. **Forster E.** *Predicting muscle forces in the human lower limb during locomotion.* Düsseldorf: VDI-Verlag, 2004.
26. **Kang KT, Koh YG, Jung M, et al.** The effects of posterior cruciate ligament deficiency on posterolateral corner structures under gait- and squat-loading conditions: a computational knee model. *Bone Joint Res* 2017;6:31-42.
27. **Kang KT, Kim SH, Son J, et al.** Probabilistic evaluation of the material properties of the in vivo subject-specific articular surface using a computational model. *J Biomed Mater Res B Appl Biomater* 2017;105:1390-1400.
28. **Kim YS, Kang KT, Son J, et al.** Graft extrusion related to the position of allograft in lateral meniscal allograft transplantation: biomechanical comparison between parapatellar and transpatellar approaches using finite element analysis. *Arthroscopy* 2015;31:2380-91.e2.
29. **Koh YG, Son J, Kwon SK, et al.** Preservation of kinematics with posterior cruciate-, bicruciate- and patient-specific bicruciate-retaining prostheses in total knee arthroplasty by using computational simulation with normal knee model. *Bone Joint Res* 2017;6:557-565.
30. **Piefer JW, Pflugner TR, Hwang MD, Lubowitz JH.** Anterior cruciate ligament femoral footprint anatomy: systematic review of the 21st century literature. *Arthroscopy* 2012;28:872-881.
31. **Hwang MD, Piefer JW, Lubowitz JH.** Anterior cruciate ligament tibial footprint anatomy: systematic review of the 21st century literature. *Arthroscopy* 2012;28:728-734.
32. **Bowman KF Jr, Sekiya JK.** Anatomy and biomechanics of the posterior cruciate ligament, medial and lateral sides of the knee. *Sports Med Arthrosc Rev* 2010;18:222-229.
33. **Baldwin JL.** The anatomy of the medial patellofemoral ligament. *Am J Sports Med* 2009;37:2355-2361.
34. **Amis AA, Firer P, Mountney J, Senavongse W, Thomas NP.** Anatomy and biomechanics of the medial patellofemoral ligament. *Knee* 2003;10:215-220.
35. **Baldwin MA, Clary CW, Fitzpatrick CK, et al.** Dynamic finite element knee simulation for evaluation of knee replacement mechanics. *J Biomech* 2012;45:474-483.
36. **Sekiguchi K, Nakamura S, Kuriyama S, et al.** Effect of tibial component alignment on knee kinematics and ligament tension in medial unicompartmental knee arthroplasty. *Bone Joint Res* 2019;8:126-135.
37. **Blankevoort L, Huiskes R.** Ligament-bone interaction in a three-dimensional model of the knee. *J Biomech Eng* 1991;113:263-269.
38. **Marra MA, Vanheule V, Fluit R, et al.** A subject-specific musculoskeletal modeling framework to predict in vivo mechanics of total knee arthroplasty. *J Biomech Eng* 2015;137:020904.
39. **Shelburne KB, Torry MR, Pandey MG.** Contributions of muscles, ligaments, and the ground-reaction force to tibiofemoral joint loading during normal gait. *J Orthop Res* 2006;24:1983-1990.
40. **Li G, Gil J, Kanamori A, Woo SL.** A validated three-dimensional computational model of a human knee joint. *J Biomech Eng* 1999;121:657-662.
41. **Rasmussen MT, Nitri M, Williams BT, et al.** An in vitro robotic assessment of the anterolateral ligament, Part 1: secondary role of the anterolateral ligament in the setting of an anterior cruciate ligament injury. *Am J Sports Med* 2016;44:585-592.
42. **Kang KT, Koh YG, Nam JH, Jung M, Kim SJ, Kim SH.** Biomechanical evaluation of the influence of posterolateral corner structures on cruciate ligaments forces during simulated gait and squatting. *PLoS One* 2019;14:e0214496.
43. **Sonnery-Cottet B, Lutz C, Dagggett M, et al.** The involvement of the anterolateral ligament in rotational control of the knee. *Am J Sports Med* 2016;44:1209-1214.
44. **Chun YM, Kim SJ, Kim HS.** Evaluation of the mechanical properties of posterolateral structures and supporting posterolateral instability of the knee. *J Orthop Res* 2008;26:1371-1376.
45. **Wang H, Fleischli JE, Zheng NN.** Transtibial versus anteromedial portal technique in single-bundle anterior cruciate ligament reconstruction: outcomes of knee joint kinematics during walking. *Am J Sports Med* 2013;41:1847-1856.
46. **Ruiz N, Filippi GJ, Gagnière B, Bowen M, Robert HE.** The comparative role of the anterior cruciate ligament and anterolateral structures in controlling passive internal rotation of the knee: a biomechanical study. *Arthroscopy* 2016;32:1053-1062.
47. **Segond P.** *Recherches cliniques et expérimentales sur les épanchements sanguins du genou par entorse.* Paris: Aux Bureaux du Progrès Medical, 1879.
48. **Dagggett M, Ockuly AC, Cullen M, et al.** Femoral origin of the anterolateral ligament: an anatomic analysis. *Arthroscopy* 2016;32:835-841.
49. **Kennedy MI, Claes S, Fuso FA, et al.** The anterolateral ligament: an anatomic, radiographic, and biomechanical analysis. *Am J Sports Med* 2015;43:1606-1615.
50. **Chen Z, Zhang X, Ardestani MM, et al.** Prediction of in vivo joint mechanics of an artificial knee implant using rigid multi-body dynamics with elastic contacts. *Proc Inst Mech Eng H* 2014;228:564-575.

Author information

- K-T. Kang, PhD, Research Professor, Department of Mechanical Engineering, Department of Mechanical Engineering, Yonsei University, Seoul, South Korea.
- Y-G. Koh, MD, Orthopaedic Surgeon, Joint Reconstruction Center, Department of Orthopaedic Surgery, Yonsei Sarang Hospital, Seoul, South Korea.
- K-M. Park, MS, Researcher, Department of Mechanical Engineering, Yonsei University, Seoul, South Korea.
- C-H. Choi, MD, PhD, Professor,
- M. Jung, MD, PhD, Associate Professor,
- J. Shin, MD, Resident,

- S-H. Kim, MD, PhD, Associate Professor, Department of Orthopedic Surgery, Arthroscopy and Joint Research Institute, Yonsei University College of Medicine, Seoul, South Korea.

Author contributions

- K-T. Kang: Designed the study, Evaluated the result using computational simulation, Wrote the manuscript.
- Y-G. Koh: Designed the study, Wrote the manuscript.
- K-M. Park: Performed the modelling.
- C-H. Choi: Evaluated the result using computational simulation.
- M. Jung: Analyzed the data.
- J. Shin: Analyzed the data.
- S-H. Kim: Corresponding author, Supervised the study.
- K-T. Kang and Y-G. Koh contributed equally to this study.

Funding statement

- No benefits in any form have been received or will be received from a commercial party related directly or indirectly to the subject of this article.

Ethical review statement

- Approval was obtained from the Yonsei University Gangnam Severance Hospital Institutional Review Board (3-2016-0271).

© 2019 Author(s) et al. This is an open-access article distributed under the terms of the Creative Commons Attribution Non-Commercial No Derivatives (CC BY-NC-ND 4.0) licence, which permits the copying and redistribution of the work only, and provided the original author and source are credited. See <https://creativecommons.org/licenses/by-nc-nd/4.0/>.